Multiscale Inefficiency Index

August 11, 2025

Abstract

This paper investigates the long-term memory and multifractal properties of financial time series through Hurst exponent estimation techniques, including both the classical R/S statistic and its modified version (M-R/S). Recognizing the limitations of a single static Hurst exponent often distorted by trends, sample length, or structural breaks we complement our analysis with Multifractal Detrended Fluctuation Analysis (MF-DFA), which reveals the local scaling dynamics and multifractal spectrum of the data. Building on these insights, we introduce a novel inefficiency index that integrates two key dimensions: the width of the multifractal spectrum, capturing scale-invariant long-range correlations, and the deviation of a rolling Hurst exponent from the efficient market benchmark of 0.5, indicating momentum or mean-reversion. To showcase the practical value of our index, we design a long/short trading strategy that uses it to filter out false signals from the Hurst exponent, thereby improving performance compared to a traditional long/short Hurst-based approach.

1 Introduction

The Hurst exponent is a crucial tool for analyzing long-term memory and self-similarity in stochastic processes. Originally introduced by Harold Hurst in the 1950s for studying river flows, this measure has since been widely adopted in various fields such as physics, environmental science and finance. In financial markets, the Hurst exponent serves as an indicator to determine whether a time series exhibits long-range dependence (a value greater than 0.5) or mean-reverting behavior (a value less than 0.5), a value equals to 0.5 indicates that the series follows a pure random walk, characteristic of standard Brownian motion.

The most common method for estimating the Hurst exponent is through Rescaled Range (R/S) analysis, introduced by Hurst and later refined by Mandelbrot. However, the traditional R/S statistic has its limitations, particularly its sensitivity to short-term memory effects, which can obscure the detection of long-term memory. To mitigate these issues, **lo1991** proposed a modified version of the R/S statistic (M-R/S) that better accounts for short-term autocorrelation.

In this study, we apply both the R/S method and the M-R/S to estimate the Hurst exponent on financial time series and we complement our analysis with Multifractal Detrended Fluctuation Analysis (MF-DFA), which examines the local behavior of the series and characterizes its multifractal spectrum. That way we can capture the local scaling dynamics and identify the presence of multifractality, which is often indicative of complex market behaviors possibly inefficient.

The Fractional Brownian motion (fBm) is often used as a benchmark model for processes with memory, as it embodies the scaling properties and persistence typically observed in long-memory data. While fBm provides a theoretical framework for understanding these phenomena, our study focuses on practical estimation methods.

2 Literature Review

Memory diagnostics in finance revolve around R/S and its modified M-RS tests; Mandelbrot and Wallis pioneered the use of the rescaled range (R/S) statistic to detect long-term memory in geophysical and financial time series, highlighting its sensitivity to persistent and anti-persistent behaviors **mandelbrot1968**; **mandelbrot1969a**; **mandelbrot1969b**. Mandelbrot further emphasized the limitations of classical methods and the need for robust estimators in the presence of nonstationarity and structural breaks **mandelbrot1973**; **mandelbrot1979**. Moreover, **dimatteo2007** review details their scope and wavelet refinements. Kwapień show that shuffling kills multifractality, proving that inefficiency derived from the width of the spectrum stem from temporal correlations rather than heavy tails **kwapien2023**.

3 Fractional Brownian Motion

Fractional Brownian motion (fBm) is a generalization of standard Brownian motion that introduces dependence in increments, making it suitable for modeling processes with memory effects. It is a continuous-time Gaussian process $X_H(t)$ where $H \in [0, 1]$ corresponds to the Hurst exponent with the following properties:

— The process exhibits self-similarity, meaning that for any scaling factor c, $c \in \mathbb{R}^+$, the rescaled process satisfies:

$$X_H(ct) \stackrel{d}{=} c^H X_H(t). \tag{1}$$

where the symbol $\stackrel{d}{=}$ denotes equality in distribution, meaning that the statistical properties of $X_H(ct)$ and $c^H X_H(t)$ are identical.

— The increments $X_H(t) - X_H(s)$ follow a normal distribution with mean zero and variance :

$$\mathbb{E}\left[(X_H(t) - X_H(s))^2\right] = \sigma^2 |t-s|^{2H}, \tag{2}$$

where H is the Hurst exponent.

— When $H = 0.5$, fBm reduces to classical Brownian motion.

— For $H > 0.5$, the process exhibits long-term positive autocorrelation, meaning that an increase in the past tends to be followed by further increases.

— For $H < 0.5$, the process has anti-persistent behavior, where an increase in the past is more likely to be followed by a decrease.

The covariance function of fBm is given by (see Section 7.1 for demonstration):

$$C_H(t,s) = \frac{\sigma^2}{2}\left(t^{2H} + s^{2H} - |t-s|^{2H}\right), \tag{3}$$

which accounts for the dependence structure of the process. The Hurst exponent H plays a critical role in determining the smoothness and correlation properties of fBm:

— **For small H values** ($H < 0.5$), the process is highly erratic, with rapid changes and weak memory effects.

— **For large H values** ($H > 0.5$), the trajectory becomes smoother, and the process exhibits long-range dependence.

3.1 Data

The data used in this analysis is monthly and consists of the historical closing prices of five major stock market indices: the S&P 500, Russell 2000, FTSE 100, Nikkei 225, and the DAX. The data spans the period from September 10th, 1987, to February 28th, 2025.

For each index, the closing price time series was transformed using the natural logarithm to obtain a series of log prices. Additionally, a stationarity test was conducted on the log prices series using the Augmented Dickey-Fuller (ADF) test. The results indicated that all series were non-stationary, suggesting the presence of unit roots. To address this, the log prices were differentiated once, after which they exhibited stationarity (test are available in Table 1).

These differentiated log returns were then used to calculate the R/S and modified R/S statistics and estimate the Hurst exponent. The purpose of using this data is to evaluate the long-term memory properties of financial markets, which can indicate persistence or mean-reversion in market behavior.

3.2 Results

The results of the Hurst exponent estimation using the traditional R/S method are presented in Table 3.

Based on the results obtained from applying the traditional R/S method, all the series appear to exhibit long-term memory, as the Hurst exponents are consistently greater than 0.5. However, the unknown asymptotic distribution of the traditional R/S statistic prevents us from determining whether these Hurst values are statistically significant. To address this, we use the modified R/S method, comparing the statistic V to the critical values provided by **lo1991** (1.620 at the 10% level

and 1.747 at the 5% level in a one-tailed test). Our analysis shows that only one series the returns of the Russell 2000 small and mid cap (US) exhibits statistically significant persistence, for the other series, despite Hurst exponents greater than 0.5, the null hypothesis of short memory cannot be rejected.

Since it seems unrealistic to characterize series with only one static Hurst exponent as the series might be influenced by local trends, periods estimations, frequencies and to gain deeper insight into the local scaling dynamics of these series, we now turn to Multifractal Detrended Fluctuation Analysis (MF-DFA). Specifically, MF-DFA allows us to investigate the variety of local behaviors present in the time series by characterizing its multifractal spectrum. This spectrum reveals how "rough" or "smooth" different segments of the series are and indicates the prevalence of each level of irregularity. By examining the multifractal spectrum, we can determine whether the data exhibits a wide range of scaling behaviors, indicative of multifractality, or if it behaves more uniformly. This transition to MF-DFA thus provides a complementary perspective that deepens our understanding of the complex, scale-dependent dynamics governing the indices and how it relates to the Hurst exponent.

3.3 Generalized Hurst Exponent

The S&P 500 and Russell 2000 are ideal candidates for multifractal analysis. The modified R/S statistic (M-R/S) for the S&P 500 is approximately 0.501 very close to 0.5 which suggests that its dynamics are consistent with efficient market behavior. In contrast, the Russell 2000 has a modified Hurst exponent of approximately 0.588, indicating significant long-range dependencies and a less efficient market.

These discrepancies between the two series highlight their distinct scaling properties and market efficiencies. Our aim with the multifractal analysis is to capture and quantify these differences in local scaling behavior. By analyzing the multifractal spectrum of each index, we hope to match these structural discrepancies, thereby providing deeper insights into the dynamics of each market. By analyzing both the S&P 500 and Russell 2000, we gain insight into how differences in efficiency and persistence affect their multifractal characteristics. For this analysis, we will use the daily returns of the Russell 2000 index, S&P 500 index from September 10th, 1987, to February 28th, 2025 (about 10 000 data points).

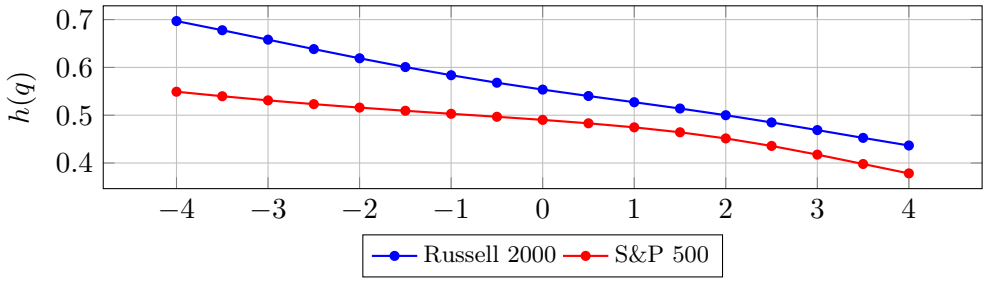

Figure 1 – Generalized Hurst exponent $h(q)$ for the S&P 500 returns. Values of q are equally spaced between -4 and 4. The scale used are logly spaced between 10 and 500.

If we take a closer look at the results from MF-DFA, we observe that the generalized Hurst exponent, $h(q)$, varies as a function of q. The decrease sloping is a sign that the serie exhibits multifractal behavior. In a monofractal process, h(q) remains constant, reflecting uniform scaling. Variation of h(q) with q indicates that small and large fluctuations scale differently. The curvature of the line indicates the presence of heterogeneity in the distribution of singularities, with different

regions of the series characterized by varying degrees of irregularity. Lower values of q emphasize small fluctuations, while higher values highlight high fluctuations. Therefore, this spectrum showcases that during periods of small fluctuations (q $<$ 0) the series is likely to exhibit long-term memory as the Hurst exponent is greater than 0.5, whether for drastic changes (q $>$ 0) in the series behavior the Hurst exponent is likely not to be high. This result is consistent with our simulation of the fractional Brownian motion (see 7.4), where we can see that the series exhibits smooth and regular behavior (calm fluctuations) for high Hurst exponent and sharply irregular behavior (high fluctuations) for low Hurst exponent.

The generalized Hurst exponent for the S&P 500 returns exhibits a similar behavior to that of the Russell 2000 returns, except that it is less pronounced. At q = -4, the series exhibits a Hurst exponent of 0.56 compared to 0.7 for the Russell 2000, those series seems to slightly differs in their behavior. This difference, albeit modest, may hint at distinct market microstructure characteristics between the two indices. For instance, the S&P 500, with its larger and more liquid companies, might experience a smoothing effect on return dynamics that could reduce the observable multifractality. In contrast, the Russell 2000, representing smaller-cap stocks, may be subject to greater fluctuations and market inefficiencies, which could amplify multifractal behavior. Overall, our findings provide an interesting perspective on market behavior, suggesting that although both indices share similar multifractal characteristics, subtle variations exist that could reflect underlying market differences.

From the MF-DFA analysis, we can also compute the Hölder exponent and multifractal spectrum. Calculating the Hölder exponent and multifractal spectrum extends MF-DFA by detailing local behavior. This logical continuation deepens insights into the complex, heterogeneous dynamics of the market.

3.4 Hölder exponent

The Hölder exponent $\alpha(q)$ characterizes the local multifractal strength of a signal and is obtained using the Legendre transform of $h(q)$:

$$\alpha(q) = h(q) + qh'(q). \tag{4}$$

where $h'(q)$ is the derivative of $h(q)$ with respect to q. This exponent quantifies the intensity of local singularities: lower values of α indicate highly irregular (or sharply singular) behavior, while higher values correspond to smoother regions of the signal. Thus, the Hölder exponent reveals the heterogeneity of fluctuations within the signal. This exponent describes the degree of multifractal in different parts of the series, revealing the heterogeneity of fluctuations.

3.5 Multifractal Spectrum

The multifractal spectrum $f(\alpha)$ provides a measure of the fractal dimension of subsets characterized by a given α:

$$f(\alpha) = q[\alpha(q) - h(q)] + 1. \tag{5}$$

This spectrum describes the distribution of singularities in the time series. A wider spectrum indicates stronger multifractality.

The analysis using the Hölder exponent and multifractal spectrum is a powerful tool for studying complex systems. In particular, it enables one to identify and quantify regions of strong multifractal, which may correspond to extreme events or sudden changes in dynamics and to describe the distribution and frequency of irregular behaviors in time series. Thus, the multifractal approach offers a detailed and nuanced description of a signal's local variability, providing essential insights for understanding and predicting its underlying dynamics.

We can distinguish two main contributions to the multifractal spectrum:

$$\mathcal{M}(q) \propto \underbrace{f_{\text{tail}}(q)}_{\substack{\text{Strongly non-Gaussian} \\ \text{distribution}}} \quad \textit{and} \quad \underbrace{f_{\text{corr}}(q)}_{\substack{\text{Temporal correlations} \\ \text{in the series}}}$$

Therefore, in the literature, the multifractality is often reffered as two types :

Type I multifractality arises from a broad probability density function of the series values **kantelhardt2002** whereas Type II multifractality stems from long-range correlations within the time series. This distinction enables us to identify and quantify the type of multifractality present. By shuffling the series, we effectively eliminate the long-range correlations, retaining only the influence of the value distribution. By using a phase randomization algorithm we can generate a surrogate which keeps the long term correlation in the series intact and make the distribution gaussian. The difference in width between spectrums showcase the degree of multifractality and hence inefficience of both sources.

The multifractal spectrum $f(\alpha)$ for the Russell 2000 (see Figure 5) returns exhibits a bell-shaped curve, indicating multiple scaling behaviors in the data. Furthermore, the approximate symmetry of the curve around its maximum implies that both large and small fluctuations are represented, albeit with varying intensity. Overall, this bell-shaped spectrum underscores the complex, multiscale nature of the Russell 2000 returns. Comparing it with the shuffled series, we observe that the width of the spectrum is lower than the original series, indicating that the shuffled series exhibits a more uniform behavior with less multifractality. The surrogate version of the series is narrower meaning that most of the multifractality that we observe are due to the non-gaussian distribution of returns. The multifractality linked to the non-gaussian distribution cannot be quantified as true multifractality since it's due to the finite sample size (**kwapien2023**). The only true multifractality comes from the long term correlation therefore, we use the width of the surrogate spectrum to quantifie for it.

See section 8.4 for the S&P 500 returns.

4 Inefficiency Index

4.1 Proposition of an Inefficiency Index

Market inefficiency is captured by two structural components: the width of the multifractal spectrum, $\Delta\alpha = \alpha_{\text{max surrogate}} - \alpha_{\text{min surrogate}}$, and the deviation of the rolling Hurst exponent from the efficient market value, $|H_{\text{rolling}} - 0.5|$. We define the inefficiency index as

$$I = \Delta\alpha_{\text{surrogate}} \times |H_{\text{rolling}} - 0.5|, \tag{6}$$

where $\Delta\alpha_{\text{surrogate}}$ quantifies true multifractality due to long-term correlations, any widening of this spectrum would imply inefficiency. In an efficient market, $H = 0.5$; any deviation indicates

temporal correlations, with $H > 0.5$ signaling persistence and $H < 0.5$ indicating anti-persistence. This approach combines the classical Hurst exponent (order 2) and the multifractal spectrum (all orders) for a comprehensive measure of inefficiency.

See Figure 9 for the inefficiency index I computed on indexes.

5 Trading Strategy

To emphasize the practical implications of our inefficiency index, we propose a simple trading strategy based on a rolling hurst and the index's values. The strategy is based on the ssec since given the inefficiency plot it seems like the ssec might be the most inefficient series with highest inefficiency corresponding to crises of 2008 and 2015. If we relied solely on a simple momentum or mean reversion strategy based on the Hurst exponent, we would encounter numerous false signals and often hold positions for only one or two days. This would result in high transaction costs and poor performance. The purpose of our inefficiency index is to act as a filter for the Hurst signal, allowing us to take positions only when the market is broadly inefficient across all scales. The strategy is as follows:

1. Calculate the rolling Hurst exponent H_{rolling} using a window size of 6 months via the Modified R/S method.
2. Calculate the inefficiency index I using the formula defined in Section 4.1.
3. Set a threshold for the inefficiency index, denoted as $I_{\text{threshold}}$. This threshold is set on 1.5 standard deviation based on a rolling 6 months.
4. If $I > I_{\text{threshold}}$ and Hurst < 0.5, it indicates a potential market inefficiency, and mean reversion so we take a short position in the asset, otherwise we are long.

The performance can be found in Table 4, the graphical representation respectively in Figure 11 and Figure 12. The number of position taken is reduced with our index (421 vs 443), which showcases that our inefficiency index serves as a filter for the Hurst signal, reducing the number of false signals and drastically improving the overall performance of the strategy in terms of Sharpe ratio, Annualized return and Max Drawdown.

6 Conclusion

In this paper, we examined the long-term memory and multifractal properties of major stock market indices using both traditional and modified R/S analysis alongside MF-DFA. Our findings suggest that, while most series display Hurst exponents greater than 0.5 implying some degree of persistence the modified R/S approach indicates that only the Russell 2000 exhibits statistically significant long memory. We introduce an inefficiency index that gauges how far a market departs from efficiency by combining two elements: the width of its multifractal spectrum, which captures long-range correlations revealed through surrogate analysis, and the deviation of a rolling Hurst exponent from the benchmark value of 0.5, signalling momentum or mean-reversion effects. By integrating these components, our index simultaneously quantifies directional inefficiencies and multifractal complexity across all orders. This index can serve as a filter of the Hurst signal to reduce the number of false signals and improving performance.

7 Appendix

7.1 Demonstration of the covariance of fractional Brownian motion (fBm)

The fractional Brownian motion (fBm), denoted by $X_H(t)$, is defined as a zero-mean continuous-time Gaussian process whose increments are correlated. Its covariance function is given by:

$$C_H(t,s) = \frac{\sigma^2}{2}\left(t^{2H} + s^{2H} - |t-s|^{2H}\right)$$

where $H \in (0,1)$ is the Hurst exponent.

A fractional Brownian motion $X_H(t)$ with $X_H(0) = 0$ has increments that are normally distributed with zero mean, specifically:

$$X_H(t) - X_H(s) \sim \mathcal{N}(0, \sigma^2|t-s|^{2H})$$

Given that the process is centered (zero mean), the covariance is defined as:

$$C_H(t,s) = \mathrm{Cov}(X_H(t), X_H(s)) = \mathbb{E}[X_H(t)X_H(s)]$$

Using the following algebraic identity:

$$X_H(t)X_H(s) = \frac{1}{2}\left[X_H(t)^2 + X_H(s)^2 - (X_H(t) - X_H(s))^2\right]$$

the covariance becomes:

$$C_H(t,s) = \frac{1}{2}\left(\mathbb{E}[X_H(t)^2] + \mathbb{E}[X_H(s)^2] - \mathbb{E}[(X_H(t) - X_H(s))^2]\right)$$

We have by definition of fBm:

$$\mathbb{E}[X_H(t)^2] = \sigma^2 t^{2H}, \quad \mathbb{E}[X_H(s)^2] = \sigma^2 s^{2H}, \quad \mathbb{E}[(X_H(t) - X_H(s))^2] = \sigma^2|t-s|^{2H}$$

Substituting these into our covariance expression, we get:

$$C_H(t,s) = \frac{1}{2}\left(\sigma^2 t^{2H} + \sigma^2 s^{2H} - \sigma^2|t-s|^{2H}\right)$$

Factoring out the term σ^2, we arrive at the final covariance formula:

$$\boxed{C_H(t,s) = \frac{\sigma^2}{2}\left(t^{2H} + s^{2H} - |t-s|^{2H}\right)}$$

This covariance function entirely characterizes the dependence structure of fractional Brownian motion, revealing long-term correlation when $H > 0.5$ (persistence) and anti-correlation when $H < 0.5$ (anti-persistence). To comeback where you left off, see Section 3.

7.2 Augmented Dickey-Fuller Test

Ticker	P-Value on log prices	P-Value on log differentiated return
S&P 500	0.863	0.000
Russell 2000	0.695	0.000
FTSE 100	0.226	0.000
Nikkei 225	0.660	0.000
DAX	0.663	0.000

Table 1 – P-values from the Augmented Dickey-Fuller (ADF) test for stationarity. The P-value of log prices refers to the Augmented Dickey Fuller test (ADF) on log prices, while the P-value of log-differentiated prices indicates the ADF test on log-differentiated returns. The null hypothesis is non-stationarity. To come back where you left off, see Section 3.1

7.3 Definition (Time Domain)

A stationary process X_t is said to exhibit long-range dependence (long memory) if there exist constants

$$a \in (0, 1), \quad c > 0,$$

such that its autocorrelation function $\rho(k)$ satisfies

$$\lim_{k \to \infty} \frac{\rho(k)}{c\, k^{-\alpha}} = 1 \tag{7}$$

where $\rho(k)$ is the autocovariance function, c is a constant (V.Mignon 2003). To comeback where you left off, see Section 3.2.

7.4 Simulation of Fractional Brownian Motion

In this simulation, we aim to generate fractional Brownian motion (fBm) to better understand how the autocorrelation decays as a function of the Hurst exponent H. By simulating paths for different values of H, we can observe how the memory and persistence properties of the process vary. To generate the fractional Brownian motion (fBm), we use a Cholesky decomposition-based approach. The covariance matrix of fBm is given by (3):

where H is the Hurst exponent, which determines the degree of long-term dependence in the process.

The steps of the simulation are as follows:

1. Define a time grid of N points between 0 and T.
2. Compute the covariance matrix using (3).
3. Apply Cholesky decomposition to obtain a lower triangular matrix L.
4. Generate a vector W of standard normal random variables.
5. Obtain the fBm path by computing $X = LW$.

The params used for this simulation are N = 1000 number of points, T = 1 day, Hurst exponents $H = 0.2, 0.35, 0.5, 0.65, 0.8$, the number of lag for the autocorrelation is 40.

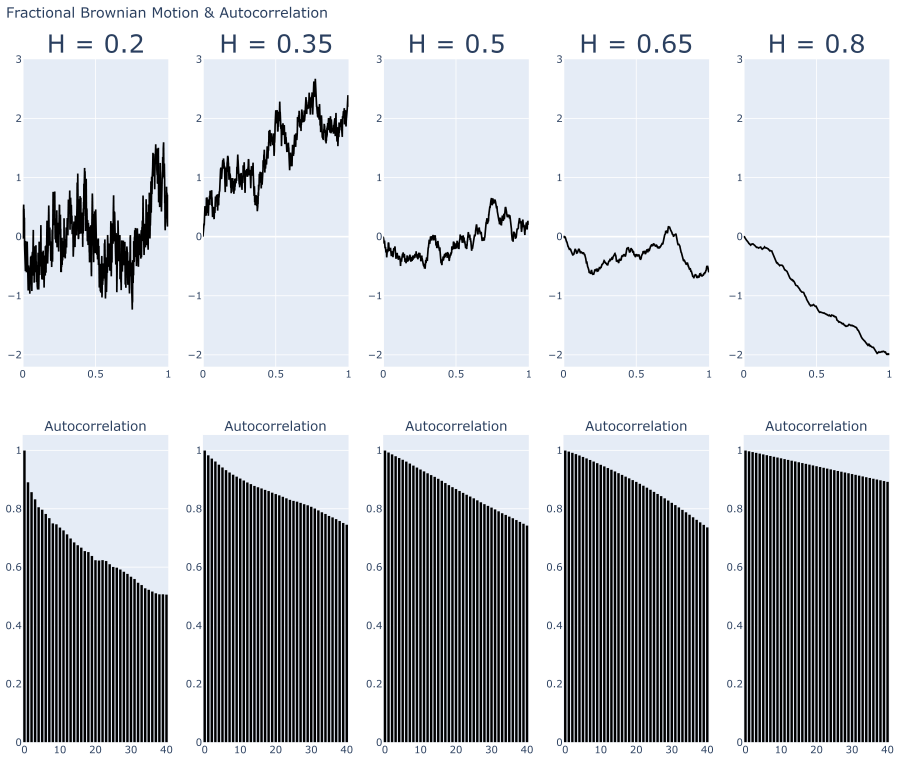

Figure 2 – Simulation of fractional Brownian motion with different Hurst exponent and its autocorrelation function. Value of H = 0.2, 0.35, 0.5, 0.65, 0.8 and 1000 points is simulated over a day.

The behavior of the fractional Brownian motion varies significantly with the Hurst exponent H.

When H is small (close to 0), the fBm exhibits high local variability, resulting in a highly granular trajectory with frequent fluctuations. The autocorrelation of increments decays rapidly, indicating that future values are weakly influenced by past values. This suggests a short-memory process, similar to standard Brownian motion.

As H increases, the autocorrelation decays more slowly, meaning that past values have a more significant impact on future values. This introduces a form of long-term dependence, where the process exhibits persistent trends. Consequently, the fBm trajectory appears smoother, with larger coherent movements and fewer abrupt changes.

In summary, a lower H leads to a more irregular and noisy path, characteristic of short-memory processes, while a higher H results in a smoother trajectory with stronger persistence.

7.5 R/S and Modified R/S Analysis

The R/S (Rescaled Range) analysis, introduced by Hurst and developed in various works by Mandelbrot, is certainly the most well-known method for estimating the Hurst exponent H. This statistic is defined as the range of the partial sums of deviations from the mean of a time series divided by its standard deviation. Consider a time series Y_t, $t = 1, \ldots, T$, with mean $\bar{Y}$. The range R is defined as:

$$R = \max_{1 \le j \le T} \left(Y_j - \bar{Y} \right) - \min_{1 \le j \le T} \left(Y_j - \bar{Y} \right). \tag{8}$$

The R/S statistic is then computed by dividing the range by the standard deviation s_T of the series:

$$Q_T = \frac{R}{s_T} = \frac{\max_{1\le j\le T}\left(Y_j - \bar{Y}\right) - \min_{1\le j\le T}\left(Y_j - \bar{Y}\right)}{s_T}, \quad \text{with } s_T = \sqrt{\frac{1}{T}\sum_{j=1}^{T}\left(Y_j - \bar{Y}\right)^2}. \tag{9}$$

Empirical studies by Mandelbrot and Wallis (1969b) have shown that Q_T scales with the number of observations T according to

$$Q_T \sim T^H, \tag{10}$$

which implies that by taking logarithms, the Hurst exponent H can be obtained from

$$H \sim \frac{\log(Q_T)}{\log(T)}. \tag{11}$$

Unfortunately, the asymptotic distribution of the R/S statistic is not known, making it difficult to establish a statistical test for the null hypothesis of short memory against the alternative hypothesis of long memory. Moreover, the R/S statistic does not explicitly account for short-term autocorrelation in the data, which can inflate (or reduce) the overall range and misrepresent the true variability of the series. Standard deviation estimates likewise ignore autocorrelated structure over short horizons, compounding the bias. As a result, the R/S measure can erroneously detect long memory when, in fact, short-term effects are responsible. This shortfall motivated Lo's Modified R/S procedure.

7.6 Modified R/S Analysis

The modified R/S statistic, denoted by $\tilde{Q}_T$, is defined as:

$$\tilde{Q}_T = \frac{R}{\hat{\sigma}_T(q)}, \tag{12}$$

where

$$\hat{\sigma}_T(q) = \sqrt{\frac{1}{T}\sum_{j=1}^{T}(Y_j - \bar{Y})^2 + \frac{2}{T}\sum_{j=1}^{T} w_j(q)\left[\sum_{i=j+1}^{T}(Y_i - \bar{Y})(Y_{i-j} - \bar{Y})\right]}, \tag{13}$$

and

$$w_j(q) = 1 - \frac{j}{q+1}. \tag{14}$$

This statistic differs from the traditional R/S statistic only by its denominator. In the presence of autocorrelation, the denominator does not solely represent the sum of the variances of the individual terms, but also includes autocovariances weighted according to lags q, with the weights $w_j(q)$ suggested by Newey and West (1987). Moreover, Andrews (1991) proposed a rule for choosing q:

$$q = [k_T] \quad \text{where} \quad k_T = \left(\frac{3T}{2}\right)^{\frac{1}{3}}\left(\frac{2\rho_1}{1-\rho_1^2}\right)^{\frac{2}{3}}, \tag{15}$$

where $[k_T]$ is the integer part of k_T, and ρ_1 is the first-order autocorrelation coefficient.

Unlike the classical R/S analysis, the limiting distribution of the modified R/S statistic is known. The statistic V, defined by

$$V = \frac{\tilde{Q}_T}{\sqrt{T}}, \tag{16}$$

converges to the range of a Brownian bridge over the unit interval. This convergence allows one to perform a statistical test for the null hypothesis of short memory against the alternative hypothesis of long memory by referring to the critical value table provided by Lo (1991), shown in Table 2. Therefore, accepting the null hypothesis implies that the series lacks the slow-decaying dependencies characteristic of long memory processes.

7.7 Critical Values for the Modified R/S Test

The critical values for the modified R/S test are provided in the table below. These values are used to assess whether the series exhibits long memory behavior based on the modified R/S statistic.

Significance Level	**critical value (modified R/S Statistic)**
0.005	2.098
0.05	1.747
0.10	1.620

Table 2 – Critical values for the modified R/S Statistic (Lo, 1991). To come back where you left off, see Section 3.2

The following table summarizes the results of the R/S statistic, modified R/S statistic, and the estimated Hurst exponents for each of the five indices analyzed:

Ticker	R/S	Hurst Exponent	Modified Hurst Exponent	Critical Value	Long Memory
S&P 500	30.166	0.558	0.501	1.007	False
Russell 2000	51.373	0.645	0.588	1.714	True
FTSE 100	40.236	0.605	0.548	1.341	False
Nikkei 225	22.234	0.508	0.508	1.048	False
DAX	26.985	0.540	0.540	1.278	False

Table 3 – Results for R/S, Hurst exponent, modified Hurst exponent, critical value at 10%, and rejection of the null hypothesis of no long memory from 1987-09-10 to 2025-02-28. The Hurst exponent can be equal for the R/S and modified R/S methods in the case where the autocorrelation coefficients are less than zero (refer to Section 7.3), in this case we set q equal to 0 and therefore the R/S and modified R/S share the same formula. To come back where you left off, see Section 3.2

8 Multifractal Detrended Fluctuation Analysis

The Multifractal Detrended Fluctuation Analysis (MF-DFA) is a generalization of the standard Detrended Fluctuation Analysis approach designed to detect multifractality in time series (Kantelhardt et al., 2002). The procedure can be summarized in five steps, as described below:

1. **Profile construction.** Given a series $\{x_k\}_{k=1}^{N}$, we first compute its mean $\bar{x}$. Then, we build the profile

$$Z(i) = \sum_{k=1}^{i} (x_k - \bar{x}), \quad i = 1, 2, \ldots, N, \tag{17}$$

where we use $Z(i)$ instead of $Y(i)$ to avoid confusion with previous definitions. This cumulative sum helps capture the local fluctuations in the data.

2. **Division into segments.** We split the profile $Z(i)$ into $N_s \equiv \lfloor N/s \rfloor$ non-overlapping segments, each of length s. Since N may not be a multiple of s, we repeat this procedure starting from the opposite end, yielding a total of $2N_s$ segments.

3. **Detrending.** For each of the $2N_s$ segments, we fit a polynomial trend (often linear or quadratic) and subtract it from $Z(i)$ in that segment. Let $z_\nu(i)$ be the fitting polynomial in segment ν. We then define the local variance as

$$F^2\big(s,\nu\big) \;=\; \frac{1}{s}\sum_{i=1}^{s}\Big[Z\big((\nu-1)s+i\big) \;-\; z_\nu(i)\Big]^2. \tag{18}$$

   This detrending step removes possible polynomial trends in the data.

4. **Generalized fluctuation function.** For each scale s, we compute the qth-order fluctuation function,

$$F_q(s) \;=\; \left\{\frac{1}{2N_s}\sum_{\nu=1}^{2N_s}\Big[F^2\big(s,\nu\big)\Big]^{q/2}\right\}^{1/q}. \tag{19}$$

   Varying q allows us to emphasize large ($q>0$) or small ($q<0$) fluctuations.
   In the special case $q=0$, the fluctuation function is defined by a logarithmic averaging (see proof in Appendix Section 8.1):

$$F_0(s) = \exp\left(\frac{1}{4N_s}\sum_{\nu=1}^{2N_s}\ln\Big[F^2\big(s,\nu\big)\Big]\right). \tag{20}$$

5. **Scaling behavior.** Finally, on double-logarithmic axes, we examine the dependence of $F_q(s)$ on s. If

$$F_q(s) \;\sim\; s^{h(q)}, \tag{21}$$

   then $h(q)$ is called the generalized Hurst exponent. In a multifractal series, $h(q)$ varies with q, indicating different scaling behaviors for large versus small fluctuations.

For monofractal series, $h(q)$ is approximately constant for all q. In contrast, for multifractal series, $h(q)$ strongly depends on q, revealing heterogeneity in the scaling of fluctuations. For a graphical representation of the steps used in the MF-DFA, refer to Figure 3.

8.1 Proof of $F_0(s)$ as $q \to 0$

Proof of $F_0(s)$ as $q \to 0$

$$F_q(s) = \Big[\tfrac{1}{2N_s}\sum_{v=1}^{2N_s}\big(F_v^2(s)\big)^{q/2}\Big]^{1/q} \implies \ln F_q(s) = \frac{1}{q}\ln S(q),$$

where

$$S(q) = \frac{1}{2N_s}\sum_{v=1}^{2N_s} e^{\frac{q}{2}\ln F_v^2(s)}.$$

As $q \to 0$, $\ln S(q) \to 0$ and we apply L'Hôpital:

$$\lim_{q\to 0}\ln F_q(s) = \lim_{q\to 0}\frac{\ln S(q)}{q} = \left.\frac{S'(q)}{S(q)}\right|_{q=0} = \frac{1}{4N_s}\sum_{v=1}^{2N_s}\ln F_v^2(s).$$

Exponentiating:

$$F_0(s) = \exp\Big[\frac{1}{4N_s}\sum_{v=1}^{2N_s} \ln F_v^2(s)\Big] = \exp\Big[\frac{1}{2N_s}\sum_{v=1}^{2N_s} \ln F_v(s)\Big].$$

Thus $F_0(s)$ is the geometric mean of the segment fluctuations. To comeback where you left off, see Section 8.

8.2 MF-DFA Graphical Representation

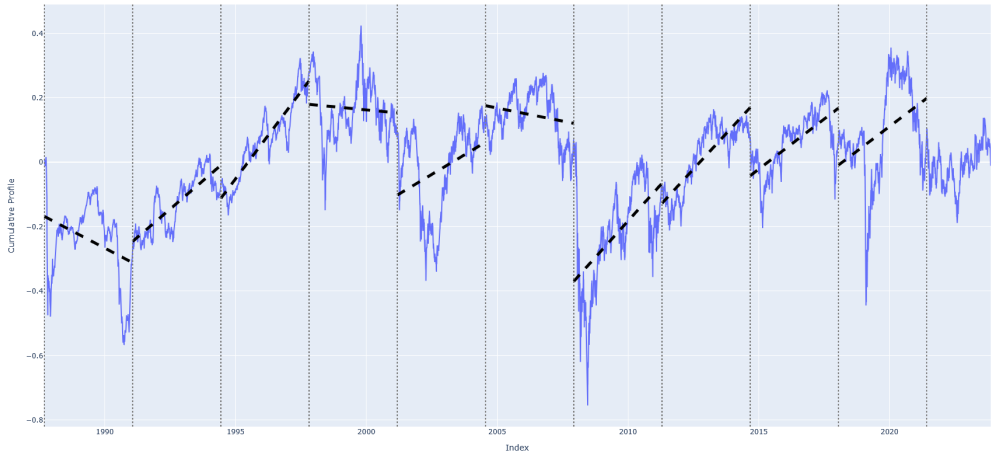

Figure 3 – Simulation of the MF-DFA steps, the series is the Russell 2000 returns split into segments of length 880. The blue line represents the cumulative sum of the centered returns, while the coloured lines represent the polynomial fit for each segment. To come back where you left off, see Section 8.

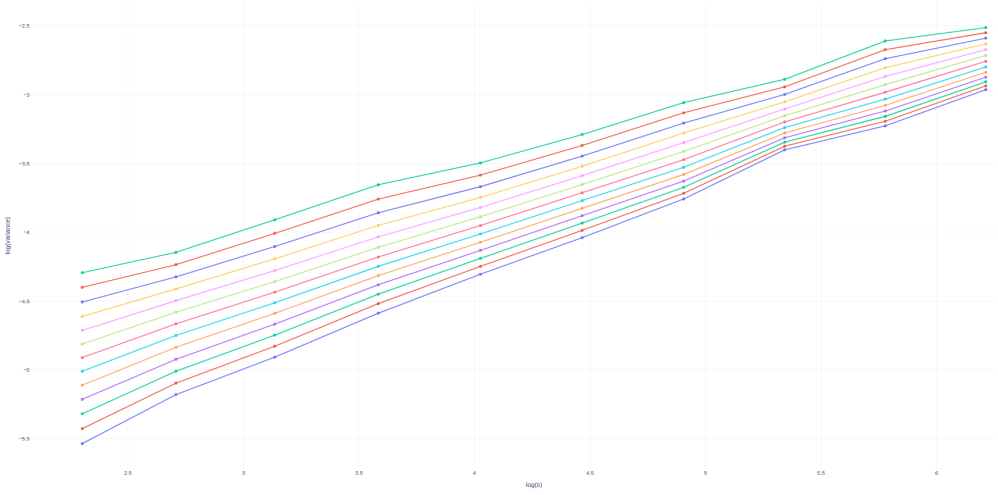

Figure 4 – Plot of the log scales (10 logly spaced increments from 10 to 500) against the log variance for each values of q, green line (highest line) represents q = -3 the lowest line represents q = 3. The slope of the line is the Hurst exponent for each q. The function is increasing with scale because, as the window size grows, larger fluctuations are aggregated, leading to higher variance.

8.3 Multifractal Spectrum of Russell Returns

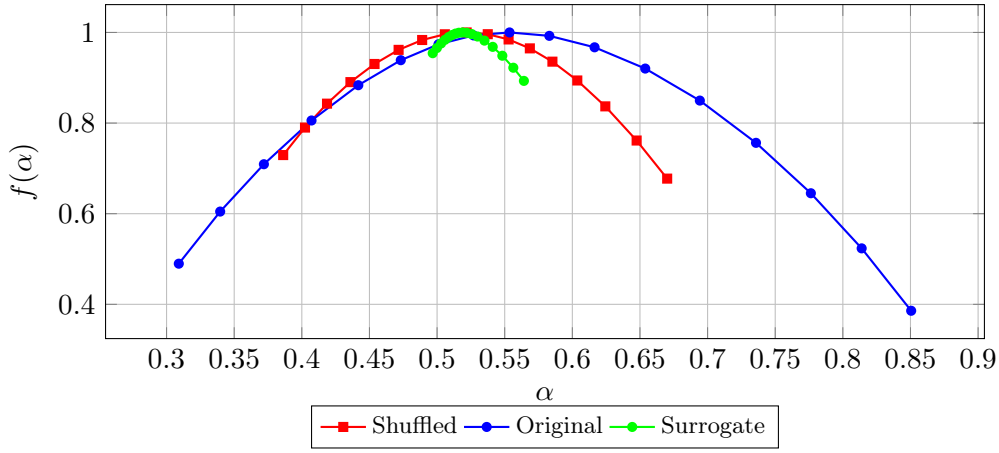

Figure 5 – Multifractal spectrum $f(\alpha)$ for the Russell 2000 returns. To comeback where you left off, see Section 3.5.

8.4 Multifractal Spectrum of S&P 500 Returns

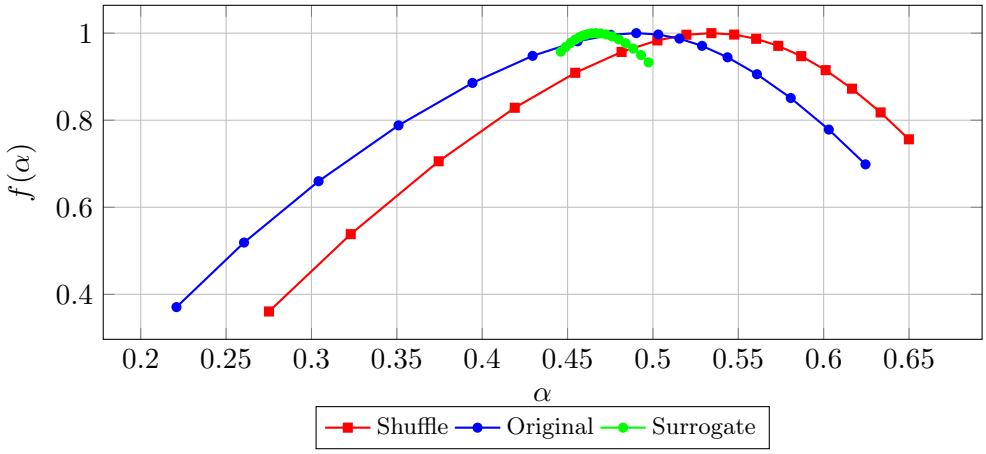

Figure 6 – Multifractal spectrum $f(\alpha)$ for S&P 500 returns.

The multifractal spectrum of the S&P 500 is noticeably narrower ($\Delta\alpha$= 0.40) and truncated on the right compared to the Russell 2000 ($\Delta\alpha$ = 0.55), pointing to a weaker multifractal signature; its central peak at α = 0.486 and an M–R/S Hurst exponent of 0.501 both underscore a near–random–walk dynamic. Unlike the Russell 2000, whose spectrum width shrinks when the series is shuffled—revealing the role of long-range correlations—the S&P 500's spectrum remains essentially unchanged by shuffling, indicating that its multifractality arises almost entirely from the non-Gaussian distribution of returns (kurtosis = 28.4). In practical terms, this means that extreme fluctuations in the S&P 500 cluster together but lack persistent temporal dependence, whereas the Russell 2000 exhibits genuine long-term memory. To come back where you left off, see Section 3.5.

9 Log Prices and Inefficiency Index

Figure 7 – Top : Log–price trajectory of the SSEC. Bottom : Inefficiency index

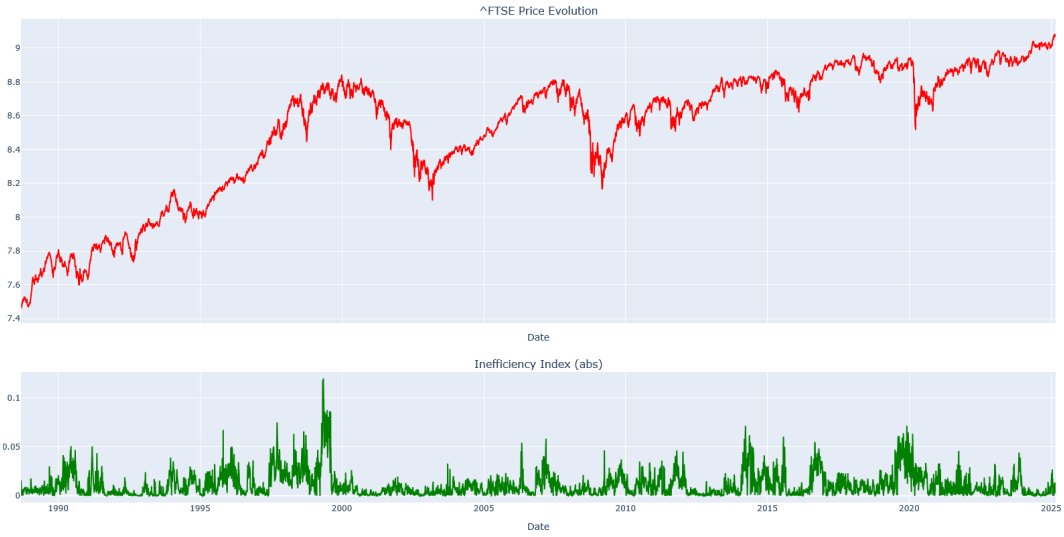

Figure 8 – Top : Log–price trajectory of the FTSE. Bottom : Inefficiency index

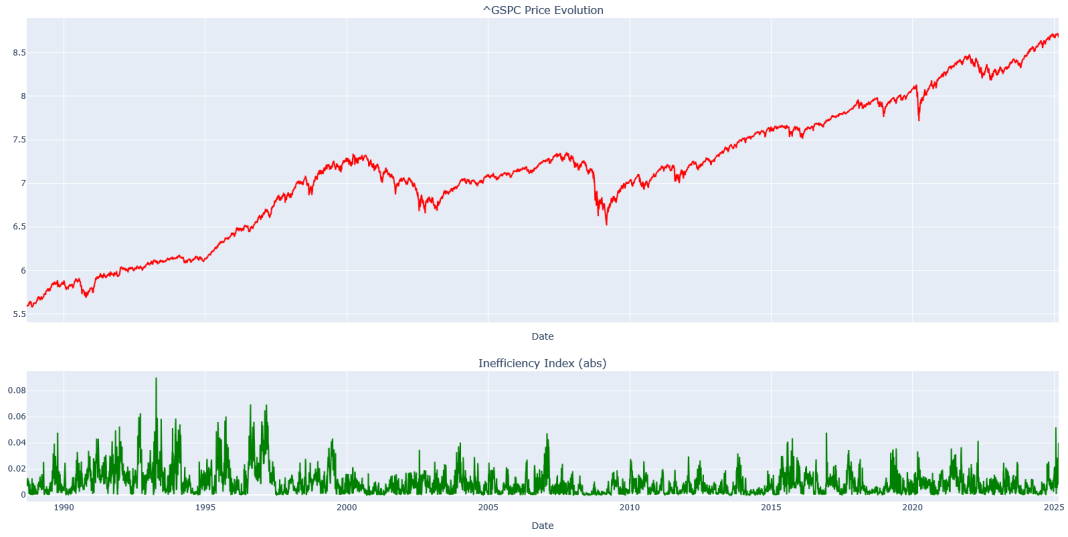

Figure 9 – Top : Log–price trajectory of the S&P 500. Bottom : Inefficiency index

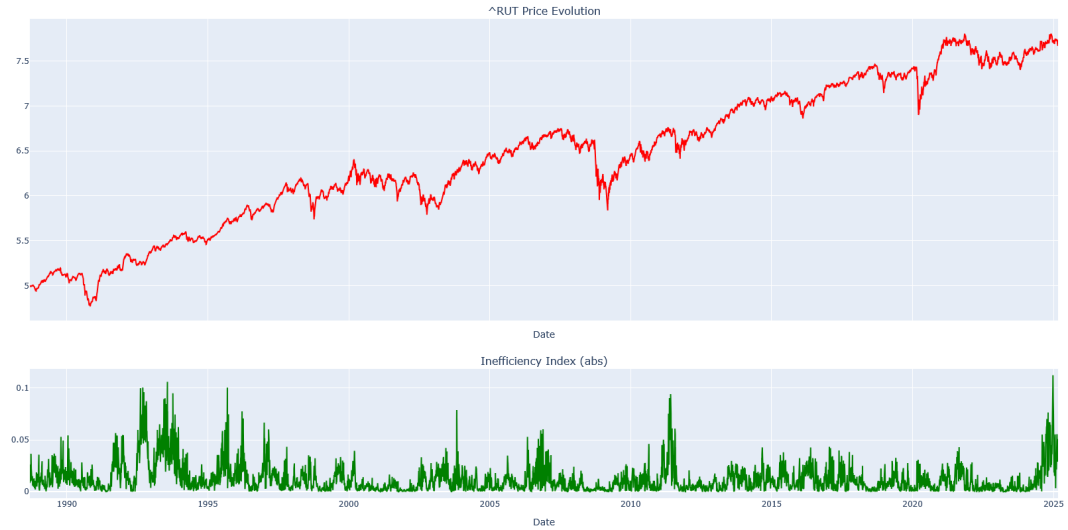

Figure 10 – Top : Log–price trajectory of the Russell 2000. Bottom : Inefficiency index

10 Trading Strategy

Strategy	Annualized Return	Annualized Volatility	Sharpe	Max Drawdown
Long/Short SSEC with inefficiency	9.521	23.307	0.409	-56.474
Long Only SSEC	3.326	23.316	0.143	-71.985
Long/short SSEC without inefficiency	5.075	23.314	0.218	-62.687

Table 4 – Performance metrics of the trading strategy with and without the inefficiency index on no transaction costs.

10.1 Cumulative Returns of the Trading Strategy

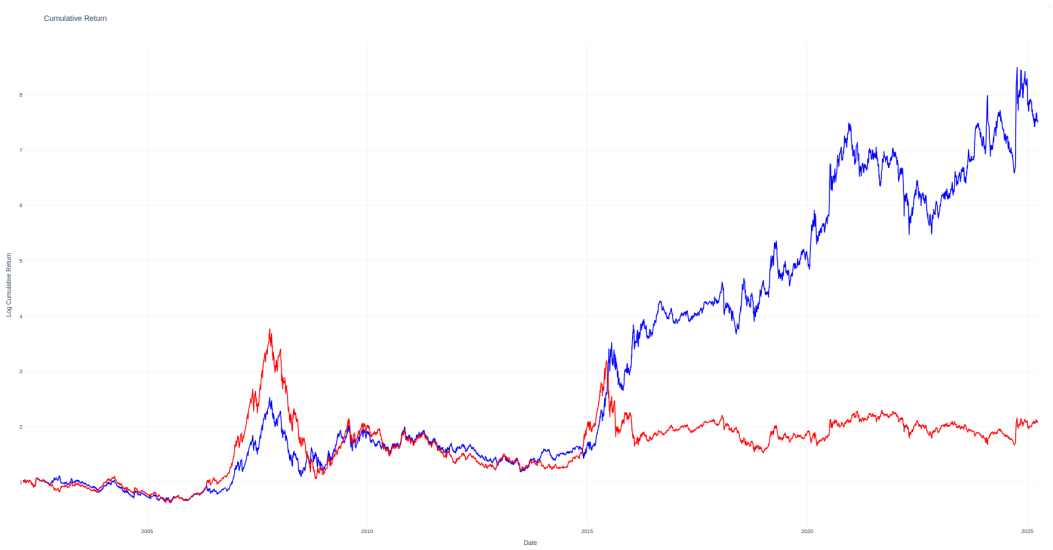

Figure 11 – Cumulative returns of the trading strategy with the inefficiency index. The blue line represents the cumulative returns of the strategy, while the red line represents the cumulative returns of the ssec. The strategy is based on the inefficiency index, which is used to filter Hurst signal.

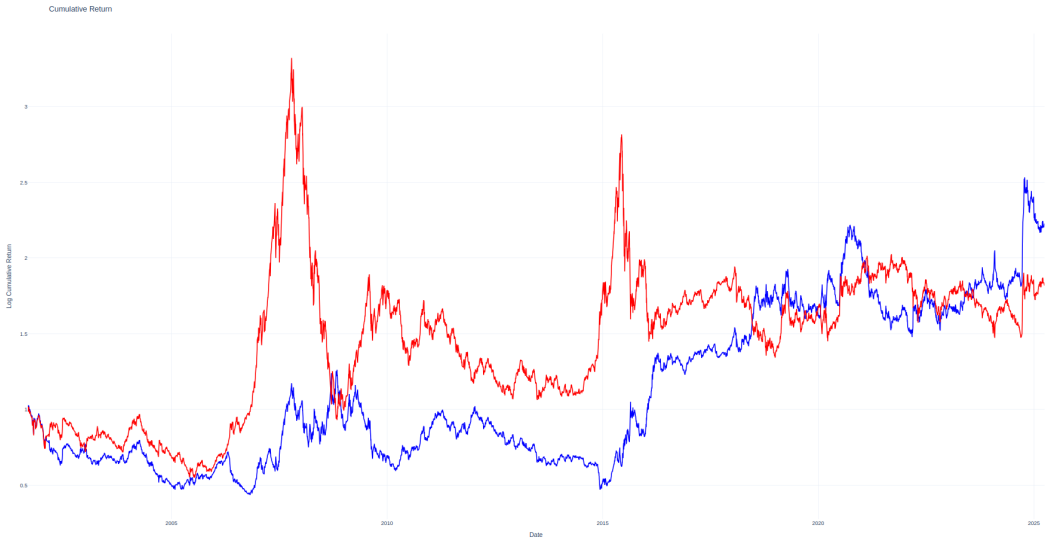

Figure 12 – Cumulative returns of the trading strategy without the inefficiency index. The blue line represents the cumulative returns of the strategy, while the red line represents the cumulative returns of the ssec. The strategy is long/short depending on the value of the Hurst (long > 0.5, short < 0.5), no filter are used.

11 References

Lo, A.W. (1991). *Long-Term Memory in Stock Market Prices*.

Mignon, V. (2003). *Méthodes d'estimation de l'exposant de Hurst. Application aux rentabilités boursières*, Économie & Prévision.

Kantelhardt, J.W., Zschiegner, S.A., Koscielny-Bunde, E., Bunde, A., Havlin, S., & Stanley, H.E. (2002). *Multifractal Detrended Fluctuation Analysis of Nonstationary Time Series. Physica A: Statistical Mechanics and its Applications*, 316(1–4), 87–114.

Lukasz Czarnecki, Dariusz Grech. (2009). *Multifractal dynamics of stock markets.* Acta Physica Polonica Series.

Kwapień, J., Drożdż, S., & Guhr, T. (2023). *Genuine multifractality in time series is due to temporal correlations: the effect of shuffling on multifractality.*

Andrews, D.W.K. (1991). *Heteroskedasticity and Autocorrelation Consistent Covariance Matrix Estimation*. *Econometrica*, 59(3), 817–858.

Mandelbrot, B.B. and Wallis, J.R. (1968). "Noah, Joseph, and Operational Hydrology", *Water Resources Research*, vol. 4, pp. 909–918.

Mandelbrot, B.B. (1973). "Le problème de la réalité des cycles lents et le syndrome de Joseph", *Economie Appliquée*, vol. 26, pp. 349–365.

Mandelbrot, B.B. and Wallis, J.R. (1969a). "Some Long-Run Properties of Geophysical Records", *Water Resources Research*, vol. 5, pp. 321–340.

Mandelbrot, B.B. and Wallis, J.R. (1969b). "Robustness of the Rescaled Range R/S in the Measurement of Noncyclic Long-Run Statistical Dependence", *Water Resources Research*, vol. 5, pp. 967–988.

Mandelbrot, B.B. and Taqqu, M.S. (1979). "Robust R/S Analysis of Long-Run Serial Correlation", *Bulletin of the International Statistical Institute*, vol. 48, pp. 69–104.

Di Matteo, T. (2007). *Multi-scaling in Finance.*